

# Spin Fluctuations and Frustrated Magnetism in the Multiferroic $\text{FeVO}_4$

J. Zhang<sup>1</sup>, L. Ma<sup>2</sup>, J. Dai<sup>2</sup>, Y. P. Zhang<sup>2</sup>, Z. Z. He<sup>3</sup>, B. Normand<sup>2</sup>, and Weiqiang Yu<sup>2</sup>

<sup>1</sup>*School of Energy, Power and Mechanical Engineering,  
North China Electric Power University, Beijing 102206, China*

<sup>2</sup>*Department of Physics, Renmin University of China, Beijing 100872, China and*

<sup>3</sup>*State Key Laboratory of Structural Chemistry, Fujian Institute of Research on the Structure of Matter,  
Chinese Academy of Sciences, Fuzhou, Fujian 350002, China*

(Dated: February 27, 2022)

We report  $^{51}\text{V}$  nuclear magnetic resonance (NMR) studies on single crystals of the multiferroic material  $\text{FeVO}_4$ . The high-temperature Knight shift shows Curie-Weiss behavior,  $^{51}K = a/(T + \theta)$ , with a large Weiss constant  $\theta \approx 116$  K. However, the  $^{51}\text{V}$  spectrum shows no ordering near these temperatures, splitting instead into two peaks below 65 K, which suggests only short-ranged magnetic order on the NMR time scale. Two magnetic transitions are identified from peaks in the spin-lattice relaxation rate,  $1/^{51}T_1$ , at temperatures  $T_{N1} \approx 19$  K and  $T_{N2} \approx 13$  K, which are lower than the estimates obtained from polycrystalline samples. In the low-temperature incommensurate spiral state, the maximum ordered moment is estimated as  $1.95\mu_B/\text{Fe}$ , or  $1/3$  of the local moment. Strong low-energy spin fluctuations are also indicated by the unconventional power-law temperature dependence  $1/^{51}T_1 \propto T^2$ . The large Weiss constant, short-range magnetic correlations far above  $T_{N1}$ , small ordered moment, significant low-energy spin fluctuations, and incommensurate ordered phases all provide explicit evidence for strong magnetic frustration in  $\text{FeVO}_4$ .

PACS numbers: 75.25.-j, 76.60.-k

## I. INTRODUCTION

In multiferroic materials such as  $\text{RMnO}_3$  (R: rare earths)<sup>1</sup>,  $\text{Ni}_3\text{V}_2\text{O}_8$ <sup>2</sup>, and  $\text{MnWO}_4$ <sup>3</sup>, ferroelectricity is believed to be driven by magnetism because it emerges simultaneously with a spiral magnetic order upon cooling. These materials are known as “type-II” multiferroics,<sup>4</sup> and their ferroelectricity as “improper.”<sup>5</sup> Even though such multiferroicity has to date been found only at low temperatures, it has attracted very significant research interest due to the possibilities it offers for tunable multiferroic devices. Phenomenologically, the breaking of magnetic inversion symmetry and strong Dzyaloshinskii-Moriya (DM) interactions are believed to be essential ingredients for understanding the coupling between ferroelectricity and magnetism.<sup>5</sup> Theoretically, inversion symmetry-breaking is thought to be caused by strong magnetic frustration. Experimentally, while magnetic frustration is certainly suggested by the available susceptibility data,<sup>6</sup> the coupling between ferroelectricity and magnetism has been difficult to quantify, and more spectroscopic studies are required to confirm its existence and explore its origin.

$\text{FeVO}_4$  is a multiferroic compound that has been characterized mostly in polycrystalline<sup>7–9</sup> or thin-film form,<sup>10,11</sup> although single crystals have also been synthesized.<sup>6</sup> It crystallizes in a triclinic structure, with each unit cell containing 6  $\text{Fe}^{3+}$ , 6  $\text{V}^{5+}$ , and 24  $\text{O}^{2-}$  ions, as shown in Fig. 1. Neutron scattering studies of polycrystal powders<sup>7</sup> indicate a collinear incommensurate antiferromagnetic (AFM) order below  $T_{N1} \approx 22$  K and a non-collinear incommensurate, or spiral, AFM order below  $T_{N2} \approx 15$  K. Ferroelectricity occurs only below  $T_{N2}$ , a result found also in other type-II multiferroic materials.<sup>5</sup>

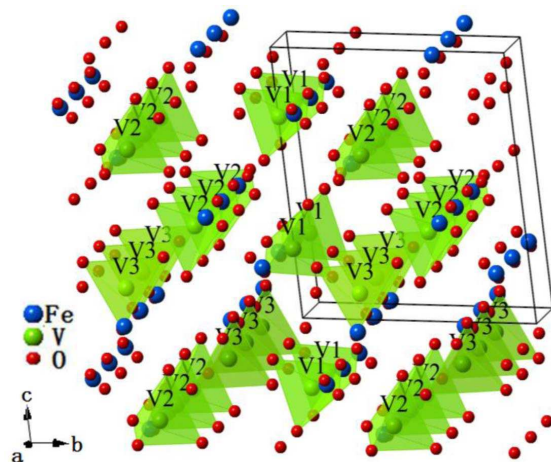


FIG. 1: (color online) Crystal structure (triclinic) of  $\text{FeVO}_4$  viewed along the  $a$  axis. The three different V sites are indicated, each occurring as a  $\text{VO}_4$  tetrahedron.

To date, however, most studies of  $\text{FeVO}_4$  have focused on this ferroelectricity,<sup>8–11</sup> and there has been only limited investigation of its magnetic states and their relation to frustration. The availability of  $\text{FeVO}_4$  as high-quality single crystals makes it an excellent target material for NMR studies of its magnetic properties and of their coupling with ferroelectricity.

NMR is a low-energy, local probe, which is in principle an ideal tool for the study of multiferroics. It is sensitive both to ferroelectricity, through the coupling between the nuclear quadrupole moment and the electric field gradient (EFG), and to magnetism, through the hyperfine coupling between the nuclei and the magnetic

moments. In  $\text{FeVO}_4$ , however, only the  $^{51}\text{V}$  signal could be observed within our available NMR window and the weak quadrupole moment ( $-0.05$  barns) of this nucleus makes the coupling to the EFG too weak to be detected. Therefore we focus primarily on the low-energy magnetic properties, which reveal strong magnetic frustration in this system, and thus also provide essential information for understanding the nature of multiferroicity.

In this paper we present all of the information about magnetism in  $\text{FeVO}_4$  that can be deduced from  $^{51}\text{V}$  NMR. The high-temperature spectrum is single-peaked in the paramagnetic phase, where the Knight shift, like the susceptibility, follows a Curie-Weiss form with a large Weiss constant. On cooling below 65 K, the spectrum splits into two peaks, which indicates a local symmetry-breaking effect on the NMR time scale, or the onset of short-range magnetic order far above the magnetic transition. From the spin-lattice relaxation time we identify the two magnetic transitions at  $T_{N1} = 19$  K and  $T_{N2} = 13$  K, consistent with other results reported on single crystals, but lower than those for powder samples. Below  $T_{N2}$ , we find a spectrum with no applied field, which reflects a complicated distribution of hyperfine fields transferred from the incommensurate magnetic moments of the Fe ions. However, the upper bound for the ordered moment is only  $1.95\mu_B/\text{Fe}$ , far less than the paramagnetic local moment, while the temperature dependence of  $1/^{51}T_1$  below  $T_{N2}$  suggests strong low-energy spin fluctuation effects. We discuss how all of these features are the fingerprints of strongly competing magnetic interactions.

The structure of our report is as follows. In Sec. II we describe briefly the NMR methods as applied to  $\text{FeVO}_4$ . In Sec. III we present all of the results we obtain for  $^{51}\text{V}$  spectra over a range of temperatures, for the relaxation times  $1/T_1$  and  $1/T_2$ , for the Knight shift  $^{51}K$ , and at zero magnetic field. In Sec. IV we discuss the implications of our results for frustrated magnetism in  $\text{FeVO}_4$  and its connection to multiferroicity. Section V contains a brief summary.

## II. MATERIAL AND METHODS

Single crystals of  $\text{FeVO}_4$  were synthesized by the flux-growth method, using  $\text{V}_2\text{O}_5$  as the self-flux.<sup>6</sup> The crystal structure is shown in Fig. 1 and the crystal alignment, required for NMR, was determined by von Laue measurements. The complete  $^{51}\text{V}$  NMR spectra were measured by field sweeps of the spin-echo signal, using a fixed frequency of 111.7 MHz and sweeping the magnetic field with its orientation parallel to the (0 1 -1) plane of the crystal. The spin-echo pulse sequence was  $\pi/2 - \tau - \pi$ , with  $\tau = 10 \mu\text{s}$  and respective  $\pi/2$  and  $\pi$  pulse lengths of 2.5 and 4  $\mu\text{s}$ . The Knight shift was determined in the paramagnetic state from  $^{51}K = (f - ^{51}\gamma B)/^{51}\gamma B$ , where  $f$  is the resonance frequency,  $B$  is the applied field, and  $^{51}\gamma = 11.197 \text{ MHz/T}$  is the  $^{51}\text{V}$  gyromagnetic ratio.

The spin-lattice relaxation rate  $^{51}T_1$  was measured by the spin-inversion method, and the spin-spin relaxation rate  $^{51}T_2$  from the spin echoes, both of which were found to follow standard, single-exponential spin recovery/decay functions.

Two comments are in order on the  $^{51}\text{V}$  spectrum at  $T = 140$  K, shown in Fig. 2(a), which has a finite Knight shift  $^{51}K \sim 3\%$ . First, from the triclinic crystal structure shown in Fig. 1, three  $^{51}\text{V}$  resonance peaks are expected. Each unit cell in  $\text{FeVO}_4$  contains three pairs of non-identical  $\text{V}^{5+}$  sites, each linked by lattice inversion symmetry and labeled by V1, V2, and V3. All three types of site have different bond lengths to all of their neighboring  $\text{O}^{2-}$  and  $\text{Fe}^{3+}$  ions, and therefore should appear as separate peaks. However, in our data only one of the three site pairs is detected within the NMR window. As we will show in Sec. III, the spin-spin relaxation time  $T_2$  of our signal is very short (less than 50  $\mu\text{s}$ ) due to the dominance of magnetic fluctuations. Thus we believe our inability to observe the other two  $^{51}\text{V}$  pairs arises because these sites have a stronger hyperfine coupling and therefore even shorter  $T_2$  times, which move the corresponding signals out of our measurement window. Second, we did not find measurable quadrupolar effects on the resonance frequency, which is reasonable for the center site of the local  $\text{VO}_4$  tetrahedra and for the low quadrupole moment of  $^{51}\text{V}$ . As noted in Sec. I, the absence of significant quadrupole effects prevents us from studying the lattice structure, and therefore the ferroelectricity, directly.

## III. NMR MEASUREMENTS

We begin our investigation of the NMR response of  $\text{FeVO}_4$  single crystals by considering the high-field  $^{51}\text{V}$  spectra at elevated temperatures. Spectra starting at 140 K are shown in Fig. 2(a). Between 140 K and 80 K they show a single peak at a field of 9.66 T, which is a regular paramagnetic signal. As we decrease the temperature to 1.5 K, it is clear that the line shape, line width, and peak frequency change dramatically, reflecting a rich variety of magnetic properties for a single material. We note that a spurious  $^{51}\text{V}$  signal is also observed at 10.0 T ( $^{51}K = 0$ ), which has a  $T_1$  value more than three orders of magnitude higher than the other peaks and does not sense the magnetic transitions on cooling, and thus is probably the consequence of a weak impurity phase or an inclusion of the crystal-growth flux. A weak and asymmetric shoulder feature at 9.65 T is also visible at temperatures between 40 and 80 K before being lost as the spectrum broadens, and this may reflect some dilute local disorder.

Figure 2(a) shows representative spectra in all of the different magnetic phases of  $\text{FeVO}_4$ . Below a temperature  $T^* = 65$  K, the  $^{51}\text{V}$  spectrum broadens and develops a prominent double-peak feature suggestive of strong spin correlations, or short-range magnetic order on the NMR time scale; we discuss this interpretation in detail

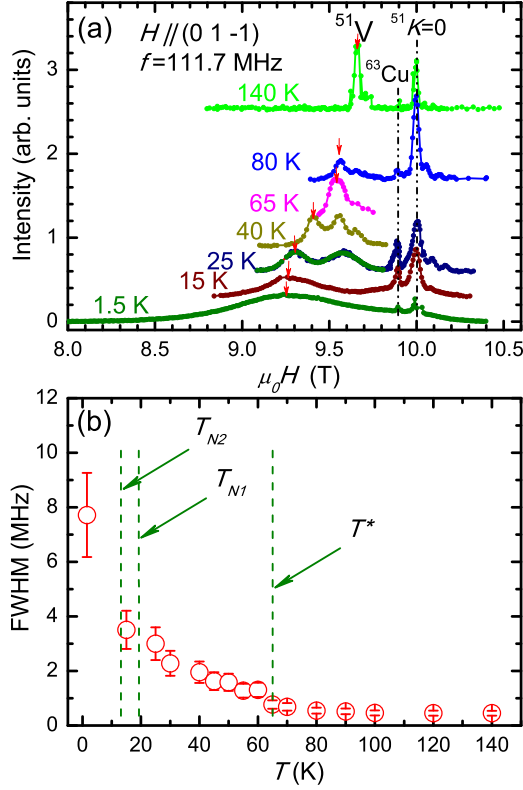


FIG. 2: (color online) (a) Field-sweep  $^{51}\text{V}$  spectra over the full range of temperatures probed, with the field applied parallel to the crystal (0 1 -1) planes. Red arrows indicate the fields used for the  $1/^{51}T_1$  and  $1/^{51}T_2$  measurements shown in Fig. 3. The solid line at 25 K is a double-Gaussian fit to the spectrum. (b) FWHM of the NMR spectra measured under the same field-sweep conditions. The temperatures  $T^*$ ,  $T_{N1}$ , and  $T_{N2}$  are introduced in the text. Vertical bars on the data points indicate the standard deviations of the fitting curves.

below. The spectra at 15 K and at 1.5 K show such significant broadening that they again appear to have a single peak. This form is typical for systems with spatially inhomogeneous magnetic order when subject to an applied field, because the nuclei respond to both the external field and the varying internal field in the crystal. We recall here (Sec. I) that at 15 K the system is in the collinear incommensurate AFM phase while at 1.5 K it is in the incommensurate spiral AFM phase. The full width at half-maximum height (FWHM) of the peak, shown in Fig. 2(b), quantifies the increase in broadening with cooling as the sample steps through the sequential changes of magnetic properties.

To identify the magnetic transition temperatures, we measured the spin-lattice relaxation rate  $1/^{51}T_1$  and the spin-spin relaxation rate  $1/^{51}T_2$ . We show results for both quantities, measured for each temperature at the peak positions on the low-field side of the spectra [red arrows in Fig. 2(a)]; below  $T_{N2}$ ,  $1/^{51}T_1$  is lowest at the peak frequency and increases by approximately 30% across the

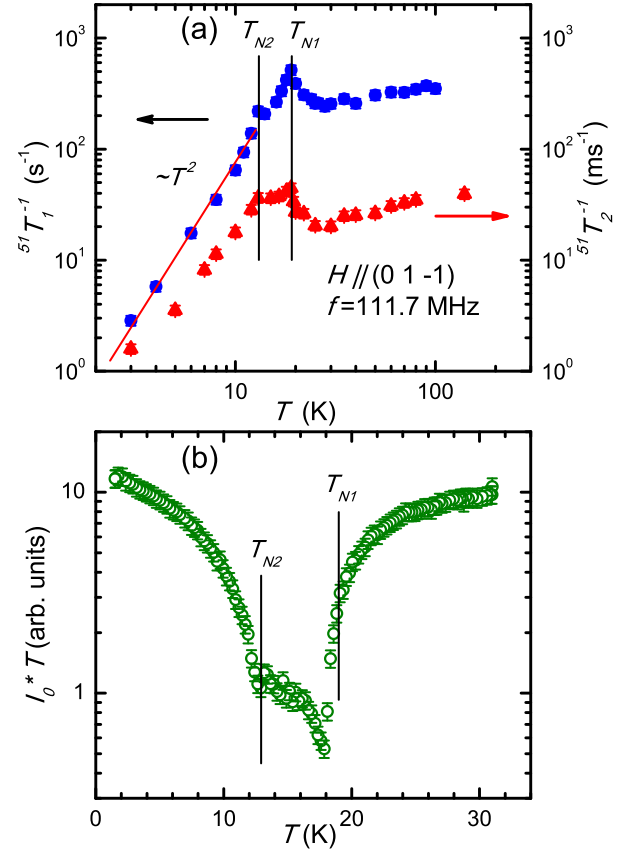


FIG. 3: (color online) (a) Spin-lattice relaxation rate  $1/^{51}T_1$  and spin-spin relaxation rate  $1/^{51}T_2$  as functions of temperature, measured at the peak position of the spectra. (b) Temperature dependence of the Boltzmann-normalized echo intensity at the peak position of the  $^{51}\text{V}$  spectrum.

frequency range. The temperature dependence of  $1/^{51}T_1$ , shown in Fig. 3(a), first displays a slow decrease with temperature upon cooling below 100 K. However, there is a prominent increase below 30 K leading to a peak at 19 K, which indicates the first magnetic phase transition at  $T_{N1}$ . Upon further cooling,  $1/^{51}T_1$  decreases again, although a small second peak is resolvable at  $T = 13$  K, indicating the second magnetic transition ( $T_{N2}$ ). Both transitions can also be resolved in the  $1/^{51}T_2$  data, also shown in Fig. 3(a), where  $1/^{51}T_2$  exhibits the same behavior as  $1/^{51}T_1$ ; two peaks in the relaxation rate are clearly formed at the two magnetic transition temperatures  $T_{N1} = 19$  K and  $T_{N2} = 13$  K. While  $1/T_1$  in a magnetic system is expected to be controlled by spin fluctuations, this is in general not so clear for  $1/T_2$ . However, the fact that  $1/^{51}T_2$  peaks at the transitions and shows a temperature dependence so similar to that of  $1/^{51}T_1$  indicates that  $1/^{51}T_2$  is indeed dominated by the magnetic fluctuations in  $\text{FeVO}_4$ . We comment again here that the  $^{51}T_2$  values shown in Fig. 3(a) are very short (under  $50 \mu\text{s}$  over much of the temperature range), a result we ascribe to these very strong magnetic fluctuations and which we

believe prevents our detection of the other two V site pairs (Sec. II).

To verify the nature of both transitions we have also measured the echo intensity  $I_0$  at the peak frequency, integrated over a finite frequency range. The Boltzmann-corrected echo intensity,  $I_0 T$ , is shown in Fig. 3(b) and is inversely proportional to both FWHM and  $e^{2\tau/T_2}$ , where  $\tau$  is the spin-echo refocusing time. As the temperature is lowered from 30 K to  $T_{N1}$ ,  $I_0 T$  decreases strongly due to the combination of inhomogeneous line-width broadening [Fig. 2(b)] and the temperature dependence of  $T_2$  [Fig. 3(a)]. In fact  $^{51}T_2 \sim 20\mu\text{s}$  is very short at  $T_{N1}$  [Fig. 3(a)] because of the strong magnetic fluctuations, and this causes a large signal loss in our spin-echo measurements. The rise in echo intensity below  $T_{N1}$  is caused by the fall in  $1/^{51}T_2$  [Fig. 3(a)]. However, the increase below  $T_{N2}$  [Fig. 3(b)] occurs despite the strong spectral broadening at these temperatures [Fig. 2(b)] and cannot be explained by  $T_2$  effects alone. While the kink directly below  $T_{N2}$  is caused by the sharp fall in  $1/^{51}T_2$  [Fig. 3(a)], the continued increase in echo intensity at low temperatures, once  $T_2$  is very long again, is due to RF enhancement of the NMR signal. This phenomenon is typical in ordered magnetic systems and has also been reported in multiferroic materials such as  $\text{TbMn}_2\text{O}_5$ ,<sup>12</sup> in this compound it shows a hysteresis effect at high fields that the authors proposed may originate in a coupling between the AFM domain walls and ferroelectric domain walls. In  $\text{FeVO}_4$  we do not find evidence for hysteresis effects, and we suggest that the RF enhancement below  $T_{N2}$  is intrinsic in a spiral magnet.

#### IV. MAGNETIC PROPERTIES

In this section we discuss the distinctive magnetic properties of  $\text{FeVO}_4$  revealed by NMR in the different regimes of temperature. We focus first on the properties in the truly paramagnetic phase above  $T^* = 65$  K. Figure 4(a) shows the Knight shift,  $^{51}K$ , deduced from the peak frequency of the spectrum, as a function of temperature. The Knight shift measures the spin susceptibility of the system, and so the monotonic increase of  $^{51}K$  on cooling is consistent with paramagnetic behavior. In fact  $^{51}K(T)$  can be fitted very well by a Curie-Weiss form,  $^{51}K = A/(T + \theta)$ , with the Weiss constant  $\theta \approx 116 \pm 15$  K; the fit is shown in Fig. 4(a). In the inset we show  $^{51}K$  against the dc susceptibility (adapted from Ref. 6) with temperature as the implicit parameter, from which we estimate the hyperfine coupling constant to be  $^{51}A_{\text{hf}} \approx 9.37 \pm 0.23$  kOe/ $\mu_B$ .

Values of  $\theta$  reported in the literature show some considerable variation, with Curie-Weiss fits to susceptibility data from polycrystals giving  $\theta \approx 125$  K<sup>7</sup> and from single-crystal measurements giving  $\theta \approx 97$  K.<sup>6</sup> This spread of results may reflect an important role for domain-wall effects, a topic to which we return below. Two incontrovertible statements are that our measurements are fully

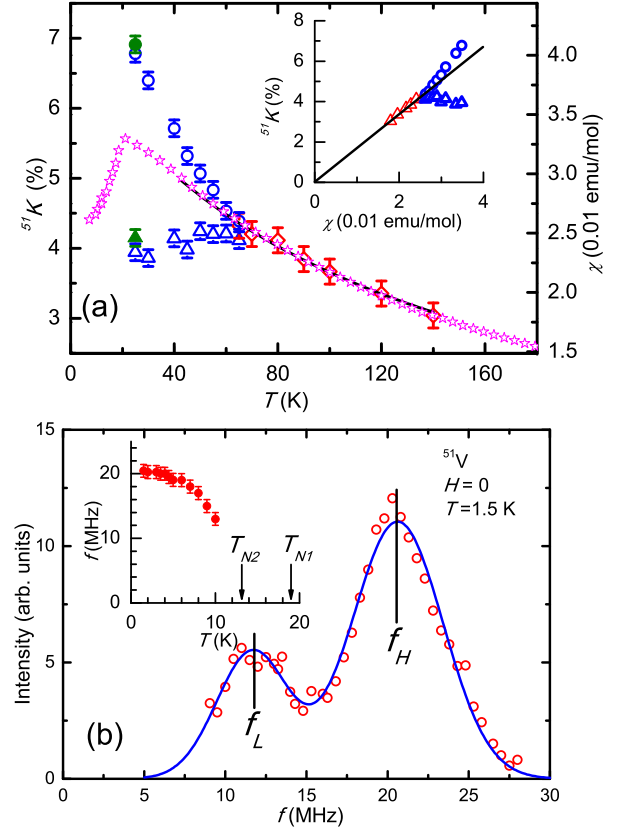


FIG. 4: (color online) (a) Temperature dependence of the Knight shift  $^{51}K$  (left axis) measured at the peak frequency of the  $^{51}\text{V}$  spectrum in the paramagnetic phase. Knight-shift data shown as open diamond, circle, and triangle symbols are measured under a field of 9.5 T, data shown as solid symbols at 4 T. The bulk susceptibility (star symbols, right axis, adapted from Ref. 6) is shown for comparison. Inset:  $^{51}K$  as a function of the dc susceptibility with temperature as the implicit parameter. Solid lines in both panels are fits to the Knight-shift data using the Curie-Weiss function. (b) Zero-field  $^{51}\text{V}$  NMR spectrum measured at  $T = 1.5$  K.  $f_H$  and  $f_L$  label the resonance frequencies of the high- and low-frequency peaks. Inset:  $T$  dependence of  $f_H$ . The arrows indicate the two magnetic transition temperatures.

consistent with previous studies and that they are consistent with  $\theta/T_{N1} \gg 1$ . Such a large value of  $\theta$  compared to  $T_{N1}$  is typical for a number of type-II multiferroic systems,<sup>5</sup> and is a key piece of evidence for strong magnetic frustration.

We turn next to the double-peak feature in the spectrum at temperatures between  $T^*$  and  $T_{N1}$ , where the intensities of the two peaks are rather similar and can be fitted rather well by a double-Gaussian function [Fig. 2(a)]. The Knight shifts calculated from both peaks are shown in Fig. 4(a), where it is clear that  $T^*$  represents a bifurcation in behavior.  $^{51}K(T)$  in this temperature range deviates both from the high- $T$  Curie-Weiss form and from the high- $T$  linear scaling with the bulk susceptibil-

ity [Fig. 4(a)]. As a consequence of this line-splitting, the overall line width of the spectral features also broadens significantly below 65 K, as shown in Fig. 2(b). We confirmed (data not shown) that the splitting of the peaks is proportional to the external field, which indicates a varying local susceptibility rather than any static magnetic ordering. Indeed, such a line-splitting is clearly a local symmetry-breaking effect, and far the most probable interpretation of our data is that the double-peak spectra are caused by strong spin correlations, or equivalently short-range magnetic ordering on the time scale of NMR. In particular, the hyperfine fields of the two V sites linked by lattice inversion symmetry may be different in this short-range-ordered state, splitting the spectrum into two peaks with equal intensity as observed. While the splitting we observe could also be caused by a breaking of crystal symmetry, no structural measurements have yet detected such a process at temperatures as high as  $T^*$ . Further evidence in favor of a short-range ordering scenario for temperatures  $T_{N1} < T < T^*$  in  $\text{FeVO}_4$  can be found by comparison with the situation when  $T < T_{N2}$ , where the magnetic order is long-ranged and static, magnetic inversion symmetry is broken,<sup>7</sup> and our zero-field NMR spectrum also resolves a double-peak feature (below).

Strong spin correlations or short-ranged magnetic order above  $T_{N1}$  in  $\text{FeVO}_4$  have been also been proposed to interpret specific-heat measurements, where a significant absence of magnetic entropy (or an “entropy recovery”) is observed over a broad temperature range above  $T_{N1}$ .<sup>6,7,10</sup> While magnetic heat-capacity measurements are complicated by issues including phonon subtraction, the line splitting and broadening we observe by NMR provide direct evidence for short-range magnetic ordering. Our results also give the first accurate measurement of the onset temperature  $T^*$ . Short-range ordering of this type has also been reported by NMR, on the basis of inhomogeneous line-width broadening, in the materials  $\text{LiCuVO}_4$ <sup>13</sup> and  $\text{LaMn}(\text{O}_{1-x}\text{F}_x)_3$ .<sup>14</sup> The appearance of short-range magnetic order in the paramagnetic state is a first indication of magnetic frustration effects, which are necessary to suppress a static AFM order in this regime. The fact that  $T^*$  is over three times the size of  $T_{N1}$ , making the short-range-ordered region remarkably broad, suggests that frustration is very strong in  $\text{FeVO}_4$ . This observation is fully consistent with the magnetic frustration revealed by the large Weiss constant in the Knight shift.

The tendency towards short-ranged magnetic order may be an important ingredient in explaining the discrepancies between Néel temperatures reported in the literature. The values we obtain from NMR,  $T_{N1} = 19$  K and  $T_{N2} = 13$  K, are consistent with the magnetization measurements also performed on single crystals.<sup>6</sup> However, values reported for powder samples<sup>7,8</sup> are  $T_{N1} = 22$  K and  $T_{N2} = 15$  K, respectively 3 K and 2 K higher, which represent a discrepancy well beyond the expected error bars of the individual measurements. We suggest that

the transition temperatures in powder samples can be enhanced both by grain-boundary and domain-wall effects and by strain effects. Given that short-range magnetic ordering already occurs at 65 K, both sets of effects provide a ready source of pinning for fluctuating magnetic moments, particularly when spiral orientations are favored. Strain effects have been found to be very effective in enhancing multiferroic properties in a number of compounds.<sup>15</sup>

Next we discuss the magnetic properties in the ordered phase. In addition to our high-field NMR studies, we have also performed zero-field NMR measurements to study the magnetic structure in the non-collinear (spiral) phase below  $T_{N2}$ . In Fig. 4(b) we show the zero-field  $^{51}\text{V}$  spectrum at 1.5 K, which has a clear double-peak structure with the two maxima centered at  $f_H$  (high-frequency) and  $f_L$  (low-frequency). The broad spectrum around each peak is caused by the distribution of hyperfine fields on the V sites transferred from the Fe moments, all of which are different due to their incommensurate order (neutron scattering measurements in this phase reveal a spiral magnetic modulation period of approximately 100 nm.<sup>7</sup>). The FWHM of the high-field spectra at  $T = 1.5$  K, shown in Fig. 2(b), is approximately 8 MHz, which is considerably less than  $f_H$  and therefore indicates that the hyperfine field on the V sites is almost perpendicular to the applied external field. The NMR spectrum in incommensurate magnetically ordered states usually has a characteristic “double-horn” feature,<sup>16–18</sup> but this is obtained when the applied field is not perpendicular to the internal field. Thus in our present field configuration we are not able to distinguish between an incommensurate spin structure and other forms of modulation that also give rise to a distribution of hyperfine fields, and can state only that our broad line shapes are consistent with the known incommensurate order. This lack of specificity applies also in the short-range-ordered phase between  $T_{N1}$  and  $T^*$ , where we cannot probe the commensurate or incommensurate nature of the spin fluctuations. We comment that the incommensurate “double-horn” shape is not similar to the double-peak structures we find in either our high-field or zero-field NMR measurements [Figs. 2(a) and 4(b)].

Although the spectral intensity is higher at  $f_H$  than at  $f_L$ , we believe this difference is due primarily to the sensitivity of the NMR pick-up. This splitting of the spectrum is probably caused by the breaking of inversion symmetry in the hyperfine field on the V sites, similar to the situation we discussed (on the NMR time scale) in the short-range-ordered state, and the default expectation would be peaks of equal weight. We have also measured  $f_H$  as a function of temperature, finding [inset, Fig. 4(b)] that it increases significantly on cooling from 10 K down to 1.5 K, reflecting the development of the ordered moment. By using the value of  $^{51}A_{\text{hf}}$  measured in the paramagnetic phase, the high-frequency resonance peak ( $f_H$ ) at zero field sets an upper bound for the ordered moment, of 1.95  $\mu_B/\text{Fe}$  at  $T = 1.5$  K. In the paramagnetic phase, how-

ever, the magnetization data give a local moment of  $5.83 \mu_B/\text{Fe}$ .<sup>6</sup> Thus the ordered moment below  $T_{N2}$  is only  $1/3$  of the net moment, indicating again the effects of strong magnetic frustration even at the lowest temperatures.

Below  $T_{N2}$ , the temperature dependence of the spin-lattice relaxation rate is different from a conventional antiferromagnet,<sup>19</sup> where  $1/T_1 \sim T^3$  due to relaxation by gapless spin waves, and the temperature dependence is stronger still in the presence of magnetic anisotropy. As shown in Fig. 3(a),  $1/^{51}\text{T}_1$ , measured at high field, has power-law behavior below  $T_{N2}$  with  $1/^{51}\text{T}_1 \sim T^2$ . Similar unconventional behavior and anomalously slow spin dynamics have been measured in other frustrated magnetic systems, such as volborthite,<sup>20</sup> where they were ascribed to a very high density of available low-energy excitations. The low power-law temperature dependence found in  $\text{FeVO}_4$  would seem to indicate the presence of persistently strong low-energy spin fluctuations on top of the spiral ordered state below  $T_{N2}$ .

The small ordered moment and the strong low-energy spin fluctuations in the spiral magnetic phase reflect once again the effects of magnetic frustration in suppressing the ordered moment while enhancing spin fluctuations. Combined with the large Weiss constant and the short-range magnetic ordering at high temperatures,  $\text{FeVO}_4$  shows explicit evidence of strong frustration all across the phase diagram. Magnetic frustration in  $\text{FeVO}_4$  is clear from the structure shown in Fig. 1, where there are multiple inequivalent Fe–O–Fe and Fe–O–O–Fe paths in the system. These paths give rise to effective magnetic coupling processes, referred to respectively as superexchange and super-superexchange in the structural and magnetic study of Ref. 7, and it is reasonable to assume that these interactions compete strongly. Our data provide independent evidence reinforcing the presence of strong magnetic frustration in  $\text{FeVO}_4$ , and by extension its importance for multiferroicity in the form of ferroelectric incommensurate SDW phases.

The origin of magnetically-driven ferroelectricity in improper multiferroics is discussed in Ref. 5. Unlike the case of proper multiferroics, it does not depend on a “ $d^0$ -type” polar distortion mechanism despite the absence of orbital moments<sup>7</sup> on both  $\text{V}^{5+}$  and  $\text{Fe}^{3+}$  (which is  $d^5$ ). In fact the breaking of magnetic inversion symmetry may in itself not be a sufficient condition, as this is broken at  $T_{N1}$  in  $\text{FeVO}_4$ , i.e. in the non-ferroelectric collinear incommensurate SDW phase.<sup>7</sup> Instead a genuine spiral magnetic order is required to sustain a polar structure,<sup>5</sup> with the polarity vector required to lie in the plane of the spiral.<sup>5,8</sup> As for the microscopic mechanism responsible for this interaction, the strong coupling between the charge and spin sectors in  $\text{FeVO}_4$  has been described as a magnetoelastically mediated magnetostriction<sup>8</sup> and as a magnetoelectric coupling<sup>10</sup> whose primary origin was proposed to lie in trilinear spin-phonon interactions.<sup>11</sup> In the magnetic sector, one of the most important terms leading to frustration and incommensurate ordered phases is the Dzyaloshinskii-

Moriya interaction, which arises from spin-orbit coupling in non-inversion-symmetric bonding geometries. These interactions are generic in systems of low crystal symmetry, exactly the situation encountered in  $\text{FeVO}_4$ , where the triclinic structure has six  $\text{Fe}^{3+}$  ions (three structurally inequivalent) in each unit cell. In combination with superexchange terms, which favor collinear order unless strongly frustrated, Dzyaloshinskii-Moriya interactions often act to produce spiral magnetic order. The resulting exchange striction, or lattice relaxation in the spin-ordered state, drives a polar charge state, i.e. a ferroelectric.

Finally, we comment once again that unfortunately we were not able to perform a direct investigation of the ferroelectric properties of  $\text{FeVO}_4$  in this study. The weak quadrupole moment of  $^{51}\text{V}$  combined with the low EFG at the centers of the  $\text{VO}_4$  tetrahedra result in a coupling between  $^{51}\text{V}$  and the crystal lattice that is too small for us to detect. Ideally, future studies of  $\text{FeVO}_4$  would perform  $^{17}\text{O}$  NMR measurements on  $^{17}\text{O}$ -enriched crystals; because the O ions bridge the Fe ions and mediate the magnetic superexchange and super-superexchange interactions, they can be expected to have a much stronger quadrupolar coupling to the lattice distortion in the ferroelectric phase.

## V. SUMMARY

In summary, we have performed  $^{51}\text{V}$  NMR measurements on single crystals of  $\text{FeVO}_4$  with both zero and high applied magnetic fields. We confirm both magnetic transitions to phases of collinear incommensurate ( $T_{N1}$ ) and spiral incommensurate ( $T_{N2}$ ) magnetic order, both occurring at values lower than those found for polycrystalline samples. Our data reveal a temperature  $T^* = 65$  K marking the onset of short-ranged magnetic order on the NMR time scale. We observe a large Weiss constant ( $\theta$ ) in the Knight shift, a prominent spectral splitting accompanying the short-range correlations, small magnetic moments in the ordered phases (deduced from the hyperfine field), and strong low-energy spin fluctuations in this regime (deduced from spin-lattice relaxation times). These results provide explicit evidence for strongly frustrated exchange interactions in  $\text{FeVO}_4$ , and thus underline the importance of magnetic frustration for the occurrence of improper ferroelectricity in multiferroic materials.

## Acknowledgments

We thank Dr. C. Y. Wang and Prof. X. J. Zhou for x-ray (von Laue) measurements of the crystal alignment. Work at North China Electric Power University was supported by the NSF of China (Grant No. 11104070) and by the Scientific Research Foundation for the Returned Overseas Chinese Scholars, State Education Ministry.



Work at Renmin University of China was supported by the NSF of China (Grant Nos. 11374364, 11174365, and 11222433) and by the National Basic Research Program of China (Grant Nos. 2010CB923004, 2011CBA00112,

and 2012CB921704). Work at Fujian Institute of Research on the Structure of Matter was supported by the National Basic Research Program of China (Grant No. 2012CB921701)

- 
- <sup>1</sup> T. Kimura, T. Goto, H. Shintani, K. Ishizaka, T. Arima, and Y. Tokura, *Nature* **426**, 55 (2003).
  - <sup>2</sup> G. Lawes, A. B. Harris, T. Kimura, N. Rogado, R. J. Cava, A. Aharony, O. Entin-Wohlman, T. Yildirim, M. Kenzelmann, C. Broholm, and A. P. Ramirez, *Phys. Rev. Lett.* **95**, 087205 (2005).
  - <sup>3</sup> K. Taniguchi, N. Abe, T. Takenobu, Y. Iwasa, and T. Arima, *Phys. Rev. Lett.* **97**, 097203 (2006).
  - <sup>4</sup> D. Khomskii, *Physics* **2**, 20 (2009).
  - <sup>5</sup> S.-W. Cheong and M. Mostovoy, *Nature Mater.* **6**, 13 (2007).
  - <sup>6</sup> Z. He, J.-I. Yamaura, and Y. Ueda, *J. Solid State Chem.* **181**, 2346 (2008).
  - <sup>7</sup> A. Daoud-Aladine, B. Kundys, C. Martin, P. G. Radaelli, P. J. Brown, C. Simon, and L. C. Chapon, *Phys. Rev. B* **80**, 220402(R) (2009).
  - <sup>8</sup> B. Kundys, C. Martin, and C. Simon, *Phys. Rev. B* **80**, 172103 (2009).
  - <sup>9</sup> L. Zhao, M. P. Y. Wu, K.-W. Yeh, and M.-K. Wu, *Solid State Commun.* **151**, 1728 (2011).
  - <sup>10</sup> A. Dixit and G. Lawes, *J. Phys.: Condens. Matter* **21**, 456003 (2009).
  - <sup>11</sup> A. Dixit, G. Lawes, and A. B. Harris, *Phys. Rev. B* **82**, 024430 (2010).
  - <sup>12</sup> S. H. Baek, A. P. Reyes, M. J. R. Hoch, W. G. Moulton, P. L. Kuhns, A. G. Harter, N. Hur, and S. W. Cheong, *Phys. Rev. B* **74**, 140410 (2006).
  - <sup>13</sup> N. Büttgen, W. Kraetschmer, L. E. Svistov, L. A. Prozorova, and A. Prokofiev, *Phys. Rev. B* **81**, 052403 (2010).
  - <sup>14</sup> K. N. Mikhalev, S. A. Lekomtsev, A. P. Gerashchenko, A. Y. Yakubovskii, and A. R. Kaul, *JETP Letters* **77**, 401 (2003).
  - <sup>15</sup> J. H. Lee and K. M. Rabe, *Phys. Rev. Lett.* **104**, 207204 (2010).
  - <sup>16</sup> M. Horvatić C. Berthier, Y. Fagot-Revurat, N. Piegay, M. E. Hanson, G. Dhalenne, and A. Revcolevschi, *Physica B* **246-247**, 22 (1998).
  - <sup>17</sup> A. A. Gippius, E. N. Morozova, A. S. Moskvina, A. V. Zalesky, A. A. Bush, M. Baenitz, H. Rosner, and S.-L. Drechsler, *Phys. Rev. B* **70**, 020406(R) (2004).
  - <sup>18</sup> M. Pregelj, A. Zorko, O. Zaharko, P. Jeglič, Z. Kutnjak, Z. Jagličić, S. Jazbec, H. Luetkens, A. D. Hillier, H. Berger, and D. Arčon, *Phys. Rev. B* **88**, 224421 (2013).
  - <sup>19</sup> J. V. Kranendonk and M. Bloom, *Physica* **22**, 545 (1956).
  - <sup>20</sup> M. Yoshida, M. Takigawa, H. Yoshida, Y. Okamoto, and Z. Hiroi, *Phys. Rev. Lett.* **103**, 077207 (2009).